Received: 15 December 2023 | Revised: 15 January 2024 | Accepted: 16 January 2024

DOI: 10.1002/rcm.9714

RESEARCH ARTICLE

Rapid Communications in Mass Spectrometry WILEY

Alternative electrolyte solutions for untargeted breath metabolomics using secondary-electrospray ionization high-resolution mass spectrometry

Cedric Wüthrich | Renato Zenobi | Stamatios Giannoukos

Department of Chemistry and Applied Biosciences, ETHZ, Zurich, Switzerland

Correspondence
Stamatios Giannoukos and Renato Zenobi, Department of Chemistry and Applied Biosciences, ETHZ, Zurich, Switzerland.
Email: stamatios.giannoukos@org.chem.ethz.ch and renato.zenobi@org.chem.ethz.ch

Funding information
Ascher Trust; Agroscope, Grant/Award Number: 15668

Rationale: Secondary-electrospray ionization (SESI) coupled with high-resolution mass spectrometry is a powerful tool for the discovery of biomarkers in exhaled breath. A primary electrospray consisting of aqueous formic acid (FA) is currently used to charge the volatile organic compounds in breath. To investigate whether alternate electrospray compositions could enable different metabolite coverage and sensitivities, the electrospray dopants NaI and $AgNO_3$ were tested.

Methods: In a proof-of-principle manner, the exhaled breath of one subject was analyzed repeatedly with different electrospray solutions and with the help of a spectral stitching technique. Capillary diameter and position were optimized to achieve proper detection of exhaled breath. The detected features were then compared using formula annotation. Using an evaporation-based gas standard system, the signal response of the different solutions was probed.

Results: Principal component analysis revealed a substantial difference in features detected with $AgNO_3$. With silver, more sulfur-containing features and more unsaturated hydrocarbon compounds were detected. Furthermore, more primary amines were potentially ionized, as indicated by van Krewelen diagrams. In total, twice as many features were unique to $AgNO_3$ than for other electrospray dopants. Using gas standards at known concentrations, the high sensitivity of FA as a dopant was demonstrated but also indicated alternate sensitivities of the other electrospray solutions.

Conclusions: This work demonstrated the potential of $AgNO_3$ as a complementary dopant for further biomarker discovery in SESI-based breath analysis.

1 | INTRODUCTION

Secondary-electrospray ionization (SESI) coupled with high-resolution mass spectrometry (HRMS) for breath analysis is a noninvasive technique for real-time monitoring of the human metabolome.[1] SESI-HRMS has already been employed for biomarker discovery of obstructive sleep apnea,[2,3] chronic obstructive pulmonary disorder,[4,5] cystic fibrosis,[6,7] and asthma.[8] Additionally, SESI-HRMS breath analysis has facilitated the monitoring of citric acid cycle intermediates,[9] sleep patterns,[10] and dietary impacts on human metabolic processes.[11]

The operational principle of SESI involves the generation of charged droplets from a primary electrospray, which ionizes gaseous or aerosolized analytes.[12] Typically, the primary electrospray consists

of a 0.1% aqueous formic acid (FA) solution for a majority of SESI applications.[12] This leads to the formation of either $[M + H]^+$ ions in positive or $[M–H]^-$ ions in negative ion mode with high efficiency.[12] A few compounds are detected as protonated dimers under sufficiently high analyte concentration.[13] SESI-HRMS operates as a direct-injection technique, without a prior separation stage such that the mass spectra obtained contain a multitude of signals. The mass spectrometric data, predominantly comprising singly (de)protonated analytes, are thus easier to interpret. The soft nature of SESI[14] further assists in this interpretative process, as most of the charged analytes remain unfragmented, indicating that each peak in the spectrum likely corresponds to a singly charged analyte.

SESI exhibits a heightened sensitivity to polar compounds, such as amines,[15] and can ionize a diverse array of analytes, including heavier compounds compared to proton transfer reaction mass spectrometry.[16] SESI ionizes a broad range of analytes, from hydrocarbon compounds to amino acids,[17] with an enhanced sensitivity for polar and basic compounds.[13] Although FA-based spray solutions are widely used in SESI research, alternative electrolyte compositions are used as well. These compositions are mainly reported with research using extractive electrospray ionization. This technique can be seen as a subset of SESI analyzing aerosolized particles, and the scope of the presented work is seen as the same.[18] For the alternative spray compositions, the spray solutions contain methanol (MeOH), isopropanol, acetonitrile (ACN), or a mixture of these solvents with water with a wide variety of dopants.[19] Next to acids, such as acetic acid,[20] salts of different metals are suitable electrospray dopants.[21–23] Notably, silver in the form of $AgNO_3$ has been demonstrated to selectively ionize sulfur-containing compounds in breath if present in the spray solution.[24] Li et al. used $AgNO_3$ to determine acetonitrile levels in the breath of smokers.[21] The monitored acetonitrile has been detected as the $[ACN + Ag]^+$ adduct. Research by Swanson and coworkers has shown the potential of alkali metals (Li, Na, and K) to form adducts with compounds containing a high number of oxygen atoms.[22] NaI specifically has later been used in devices to monitor indoor or outdoor air quality aerosol content.[23,25,26]

Although these electrolyte compositions have found application in diverse fields, their integration into untargeted breath metabolomics with SESI-HRMS has not been explored. This research delineated here provides a proof of principle for the use of silver and sodium salts as alternative dopants in the primary electrospray of SESI, aiming to extend the breath metabolomics coverage beyond that afforded by standard aqueous FA solution. The investigation also elucidates the impact of a water–MeOH (50%:50%) mixture on the profile of detected breath features. The different electrolyte solutions were then further characterized using gas standards.

The presented results provide the groundwork for future breath studies employing SESI-HRMS with different electrolyte matrices to achieve a broader and more comprehensive coverage of the breath metabolome.

2 | METHODOLOGY

2.1 | Chemicals

Optima LC-MS-grade water and MeOH (both Fisher Scientific) were used for the electrospray solution. FA (0.1% v/v, purity: ≥99.99%, Sigma-Aldrich), NaI (1 mM, purity: ≥99%, Sigma-Aldrich), and $AgNO_3$ (1 mM, purity: ≥99.995%, Thermo Scientific) were utilized as spray dopants at given concentrations. For the generation of the gas standards, limonene (purity: ≥95%), eucalyptol (purity: ≥99%), isopropanol (purity: ≥99.8%), and acetone (purity: ≥99.5%) were purchased from Sigma-Aldrich. Pentanoic acid (purity: ≥99.8%) was obtained from Supelco and pyridine (purity: ≥99%) from VWR Chemicals.

2.2 | Online SESI-HRMS breath measurements

Breath of a volunteer (27-year-old healthy male) was sampled using a spirometry filter (Vyaire Medical, Germany) connected to a custom adapter. For each electrolyte solution, six exhalations were provided in each measurement, with three replicates of each measurement on separate days. This adapter was, in turn, connected to the SESI source and one exhaust port leading to a flow meter (EXHALION, Fossil Ion Tech, Spain). The SESI source (SuperSESI) was procured from Fossil Ion Tech and connected to a Q-Exactive Plus Orbitrap mass spectrometer (Thermo Fischer, Germany). The temperature of the sample inlet was maintained at 130°C and that of the ionization chamber at 90°C. The electrospray was facilitated by applying an overpressure of 0.8 bar on the vial containing the electrolyte solution. Two different electrospray emitters were employed, a nano-electrospray emitter with a 20-µm inner diameter (outer diameter = 365 µm, Fossil Ion Tech) and an emitter with a 50-µm inner diameter (outer diameter = 363 µm, BGB, USA). To optimize the signal response of breath for each electrospray solution, different distances between the emitter and the mass spectrometer's inlet were probed. These distances were adjusted to 2, 10, and 24 mm. A sheath gas flow at 15 psi and an auxiliary gas at 2 arbitrary units (a.u.) were applied to form the spray. A voltage of ±3.5 kV was applied across all measurements, depending on the ion mode. The inlet capillary of the mass spectrometer was set to a temperature of 250°C, and the radio-frequency (RF)-value of the S-lenses was set to 50 a.u. To enhance the robustness of feature detection, spectra were acquired using spectral stitching.[27] For measurements conducted with NaI and $AgNO_3$, it was assumed that the scan intervals of the FA measurements would be transferable for these adducts. Consequently, the intervals were adjusted to accommodate the anticipated adducts. The *m/z* ranges of the individual scans are presented in Table S1. Each scan was conducted at a resolution of 140 000, with an automatic control gain target of 10^6 and a maximum injection time of 500 ms.

2.3 | Gas standard measurements

A system based on controlled evaporation of a liquid analyte and its diffusion in a carrier gas stream was employed to generate gas standards.[28] The selected compounds were initially diluted in water at concentrations mentioned in Table S2. Ten microliters of the liquid stock solutions was injected into the evaporation chamber, and its headspace volume was diluted with a nitrogen stream at flow rates of 1, 2, 4, 6, 8, and 10 mL/min. Further dilution was done with a larger nitrogen flow of 8 L/min, which was either dry (~0% relative humidity) or humidified through a bubbler (~95% relative humidity). Initially, each aqueous electrospray was individually tested with different gas standards under dry and humified nitrogen dilution flows. Gas standards were generated from limonene, eucalyptol, isopropanol, acetone, propanoic acid, and pyridine. Measurements were conducted by altering the flow through the evaporation chamber on and off for 30-s intervals, escalating from 1 to 10 mL/min. For the second round of measurements, both aqueous and water–MeOH electrosprays were tested with a humidified dilution flow. A composite mixture of the aforementioned compounds was injected into the evaporation chamber. The flow rates for these experiments were sequenced as 10, 1, 8, 2, 6, and 4 mL/min. Only the intensity during the 4-mL/min flow was considered to compare the signal response.

The settings of the mass spectrometer remained consistent with those used for exhaled breath measurements, with the exception that the spectral stitching technique was not applied. The scan range for FA was set to 50–500 *m/z*, for NaI 50–523 *m/z*, and for $AgNO_3$ 106–609 *m/z* for consistency with the ranges set for exhaled breath.

2.4 | Data processing and feature annotation

The acquired mass spectra were converted to the mzML format[29] using ProteoWizard[30] and subsequently processed using a custom Python (version 3.9) script running on the Euler computer cluster at ETH Zurich. This script interpolated all spectra with a step size of 10^{-5} *m/z* and averaged all interpolated spectra into a composite mass spectrum. Peak detection within this mass spectrum employed a height filter of 100 and a minimal distance of 10^{-4} *m/z* between peaks. The corresponding peak widths were determined at 90% of their maximum height. For each measurement, the signal of each individual peak was determined by integration within their peak's boundaries, resulting in a temporal profile for each peak. These profiles were then aligned with the exhalations recorded by the flow meter. A peak was attributed to an exhalation if its average intensity was higher during exhalations than the spray baseline. If a peak matched this criterion, its average intensity was stored in an intensity matrix.

For each experimental condition, feature annotation was performed only on features detected in all three replicates. The PyC2MC package[31] was utilized for this purpose. Heuristic rules for annotation were used to assign molecular formulae to features, including the ratios between elements.[32] The elements C, H, N, O, and S were considered for all formulae. Sodium (Na) was included for features detected in NaI measurements and silver (Ag) for those in $AgNO_3$ measurements. The analyte ions were assumed to be singly charged considering only the following adducts: $[M + H]^+$, $[M + Na]^+$, and $[M + Ag]^+$. A relative *m/z* deviation of 10 ppm was allowed. All possible formulae within this deviation were considered to be valid. A final data matrix was constructed by combining the intensity of features annotated with the same molecular formulae. The dimensions of the resulting matrix were structured as experimental conditions using unique molecular formulae.

Principal component analysis (PCA) was conducted using the Scikit-learn library (version 1.3) in Python (version 3.9).[33]

3 | RESULTS AND DISCUSSION

3.1 | Mass spectra

To optimize performance across all electrolyte solutions, it was necessary to determine the ideal electrospray emitter and the precise distance between the tip of the emitter and the inlet of the mass spectrometer. For all electrolyte solutions without dopant or FA, the electrolyte solution consisting of 50% MeOH and 1 mM NaI, the emitter with a 20-µm inner diameter yielded the most intense signals. However, the emitter clogged rapidly when used with other electrolyte solutions, resulting in a swift decline in signal intensity. Conversely, the 50-µm emitter maintained consistent performance without clogging and was therefore selected for these solutions. The optimal emitter-to-inlet distance was determined based on the signal enhancement observed during exhalation, which served as an indicator of improved detection of compounds present in exhaled breath. For solutions without dopants, as well as those containing FA and NaI in a water–MeOH mixture, a distance of 2 mm was found to be the most effective. In contrast, for all silver solutions and NaI in water, a distance of 24 mm was optimal. Notably, when using $AgNO_3$, elemental silver was deposited on the tantalum electrode of the high-voltage cable, which oxidized. The deposited layer was removed after the experiments. With the optimal emitter and distance determined, repeated measurements were conducted on separate days to ensure reliability. The average mass spectra for each aqueous electrolyte solution are shown in Figure 1.

Initially, the average spectra exhibited distinct differences. The most intense peaks for the water and aqueous FA electrospray (Figure 1A,B) were an order of magnitude more pronounced than the ones observed for NaI and $AgNO_3$ spectra (Figure 1C,D). The water-only electrospray produced only a few peaks, whereas the FA electrospray revealed multiple peaks of comparable intensity. The pattern of these high-intensity peaks matches with previously reported feature distributions.[16] In the spectrum generated from the NaI-doped electrospray, only a few features were discernible until ~170 *m/z*. Beyond this point, the spectrum displayed a denser array of signals with higher-intensity signals. Notably, signals from NaI cluster ($[(NaI)_n + Na]^+$, $n = 1, 2, 3$) were discernible and could serve

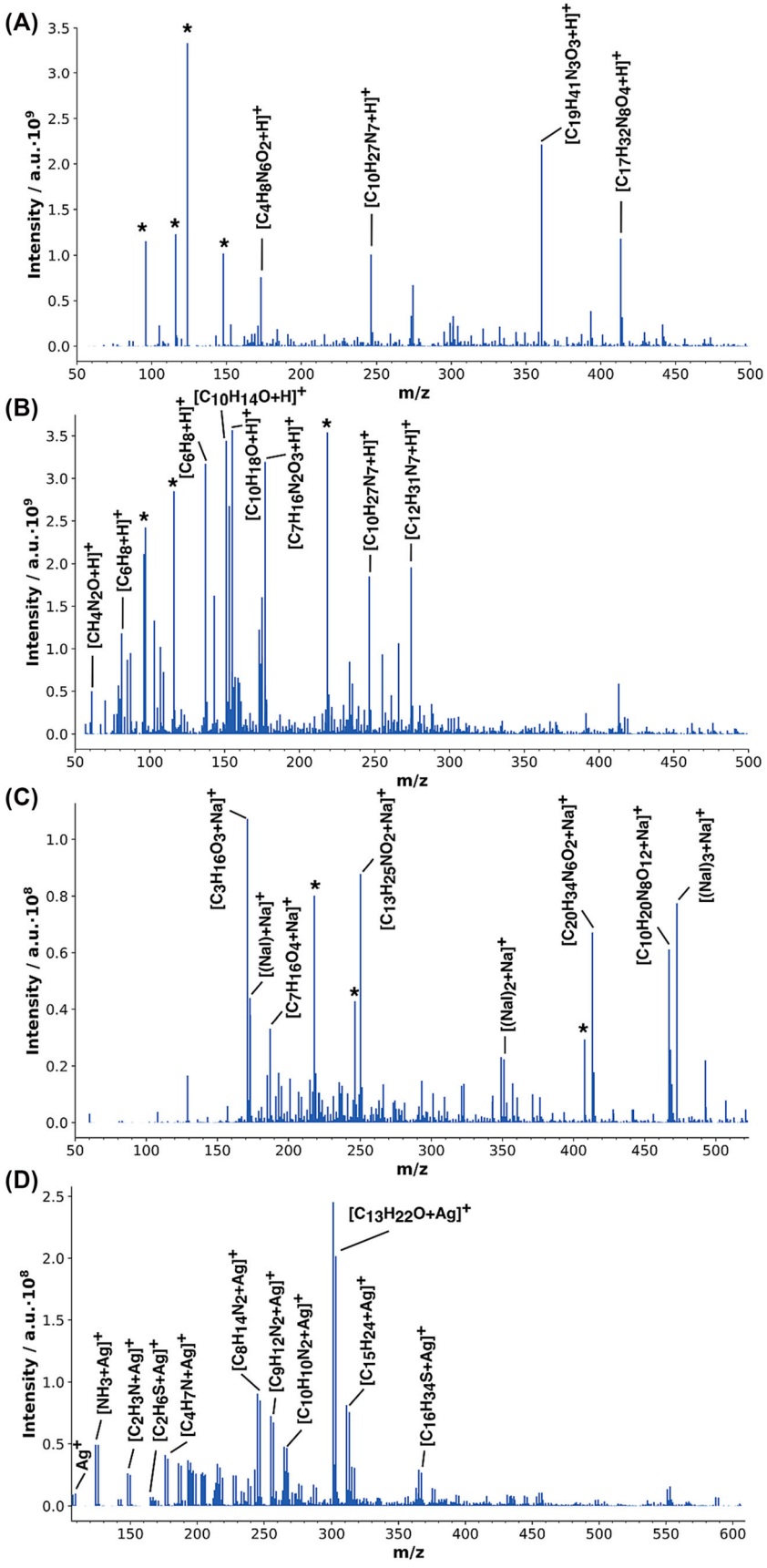

FIGURE 1 Average mass spectra derived from three replicates, each consisting of six exhalations. The intensities represent the integral beneath the signal and are comparable. The solvent for all electrolyte mixtures was pure water. (A) H_2O only, (B) FA, (C) NaI, and (D) $AgNO_3$. Annotations for the molecular formulae are provided for the most intense peaks. Asterisk (*) indicates peaks for which no annotation with the given restrictions was found. A comparative analysis of peak intensities reveals that the most intense signals were observed in the mass spectra for pure water or the aqueous formic acid electrospray. In the NaI spectrum (C), clusters denoted by $[(NaI)_n + Na]^{+}$[23] are clearly discernible. In (D), the isotopic pattern of silver is visible for the most intense peaks. [Color figure can be viewed at wileyonlinelibrary.com]

as a standard to normalize the data and ensure the precision of the *m/z*-axis.[23] In the spectrum obtained from the silver-doped electrolyte, the silver cation was clearly detectable, followed by the signals of $[NH_3 + Ag]^+$ and $[ACN + Ag]^+$. The use of silver adducts enabled the detection of these molecules using Orbitrap, with its lower mass limit of 50 *m/z* due to the heavier mass of silver. Many of the most intensive signals in the spectra were attributable to molecular formulae containing nitrogen atoms, suggesting the presence of amines. As previously reported,[24] the affinity of silver toward sulfur-containing compounds leads to the presence of the dimethylsulfide-silver adduct, as well as a heavier compound with the annotated formula $C_{16}H_{34}S$.

Although employing water as the electrospray solvent is common in SESI, a mixture of water and MeOH can be employed to enhance the extraction phase of the ionization pathway.[34] Therefore, water–MeOH solvent (50:50) mixture was used, yielding the spectra for exhaled breath as shown in Figure 2.

With the inclusion of MeOH in the spray solution, all spectra visibly changed from when pure water was used, with the exception of the $AgNO_3$-doped solution. The mass spectrum obtained from the nondoped solution (Figure 2A) was characterized by three intense peaks, whereas the rest of the spectrum contained signals with a less-intense magnitude. For both FA- and NaI-doped solutions (Figure 2B,C), the most intense peaks emerged above 250 *m/z*. This contrasts with the spectra shown in Figure 1, where the most intense peaks were below 250 *m/z* in the case of FA or more evenly distributed across the mass spectrum in the case of NaI. It could be that the additional MeOH in the spray solution enhanced the ionization efficiency of heavier compounds, which are typically associated with aerosols. Other factors that could have been responsible for the differences between the NaI spectra could be attributed to the different emitter diameters and positioning of the spray tip. The spectrum obtained from measurements with $AgNO_3$-doped electrospray solution (Figure 2D) shows minimal differences compared to the water-only solvent results (Figure 1D), suggesting that the presence of silver in the spray may not be significantly influenced by the addition of MeOH under the conditions tested.

3.2 | Feature comparison

To facilitate the comparison of the detected features under various conditions, molecular formulae were calculated from individual *m/z* peaks. Then, the intensity of each corresponding *m/z* feature was appended alongside each formula or multiple formulae, based on the number of potential candidates identified within the given relative mass error of 5 ppm. As a final product, a data matrix was obtained, with the intensity values of each molecular formula match depending on the electrolyte solution as entries. Within all recorded spectra, 4644 features were annotated with molecular formulae. Among these features, 708 were unique to the aqueous FA solution, 531 to NaI, and 1679 to $AgNO_3$. For the water–methanol (50:50) mixture, 131 were unique to FA, 180 to NaI, and 63 to $AgNO_3$.

To illustrate the feature similarities across the different conditions, PCA was conducted. The first two principal components are shown in Figure 3A, whereas the third component is shown in Figure S1.

The first principal component clearly distinguishes the data obtained with the silver-doped electrospray. The second component separates the data obtained from the electrospray containing aqueous FA. There was no evident clustering by the solvent used, which indicates that silver doping enhances the ionization of certain compounds or even makes some ionizable only in its presence. This is further supported by data shown in Figure 3B. The deconvoluted masses of the individual features are exhibited for each of the electrospray solutions alongside their signal intensity. The features detected using the silver-doped spray with or without MeOH were numerous and possessed higher molecular masses than in almost all other conditions, leading to their distinct separation in the PCA plot. The feature coverage of the FA-doped electrospray was the only one approaching that of the silver, with substantial coverage in the lower-mass range and less dense coverage at higher masses. This pattern was also reflected in the second principal component, which distinguished the data obtained from the aqueous FA electrospray. To visualize the ionized compound classes, the detected features and their closest formula matches are shown in van Krewelen diagrams (Figure 4).

The distribution of individual features across the element ratios indicated the presence of certain compound classes within the dataset. When examining the oxygen–carbon (O–C) ratio (first column, Figure 4), a notable difference was observed between FA and silver nitrate data. The area around the hydrogen–carbon (H–C) ratio of 1.5 was more densely populated in the case of silver, especially at low O–C ratios. Silver nitrate features were more numerous above an H–C ratio of 2.0. As already reported for ESI[35] or desorption electrospray ionization (DESI),[36] silver forms adducts with unsaturated hydrocarbons. Potential compound families with these ratios are furans, benzofurans, and their derivatives.[37] Another class could be lipids, which have shown enhanced detection with silver adducts using DESI[36] and are also a plausible category within the observed ratio range for biological systems.[38] Interestingly, the most intensive features detected using the NaI-doped electrospray appeared right below a H–C ratio of 2. These features clustered around an O–C ratio of 0.2, suggesting a relationship to compounds with alcohol functional groups.[22] Still, the increased coverage in this area barely outmatched the one observed with silver.

A comparison of the N–C ratios across all features revealed regions in the diagrams that were covered by Ag and, to some extent, Na but not by FA. This area contained features with high H–C ratios across the full spectrum of N–C ratios, indicative of compounds containing multiple primary amines, which would match the observed ratios.

In general, a higher number of features were found for silver data, especially those with low N–C ratios. Unsurprisingly, a greater number of features annotated with sulfur-containing formulae were detected with the silver-doped electrospray compared to the other

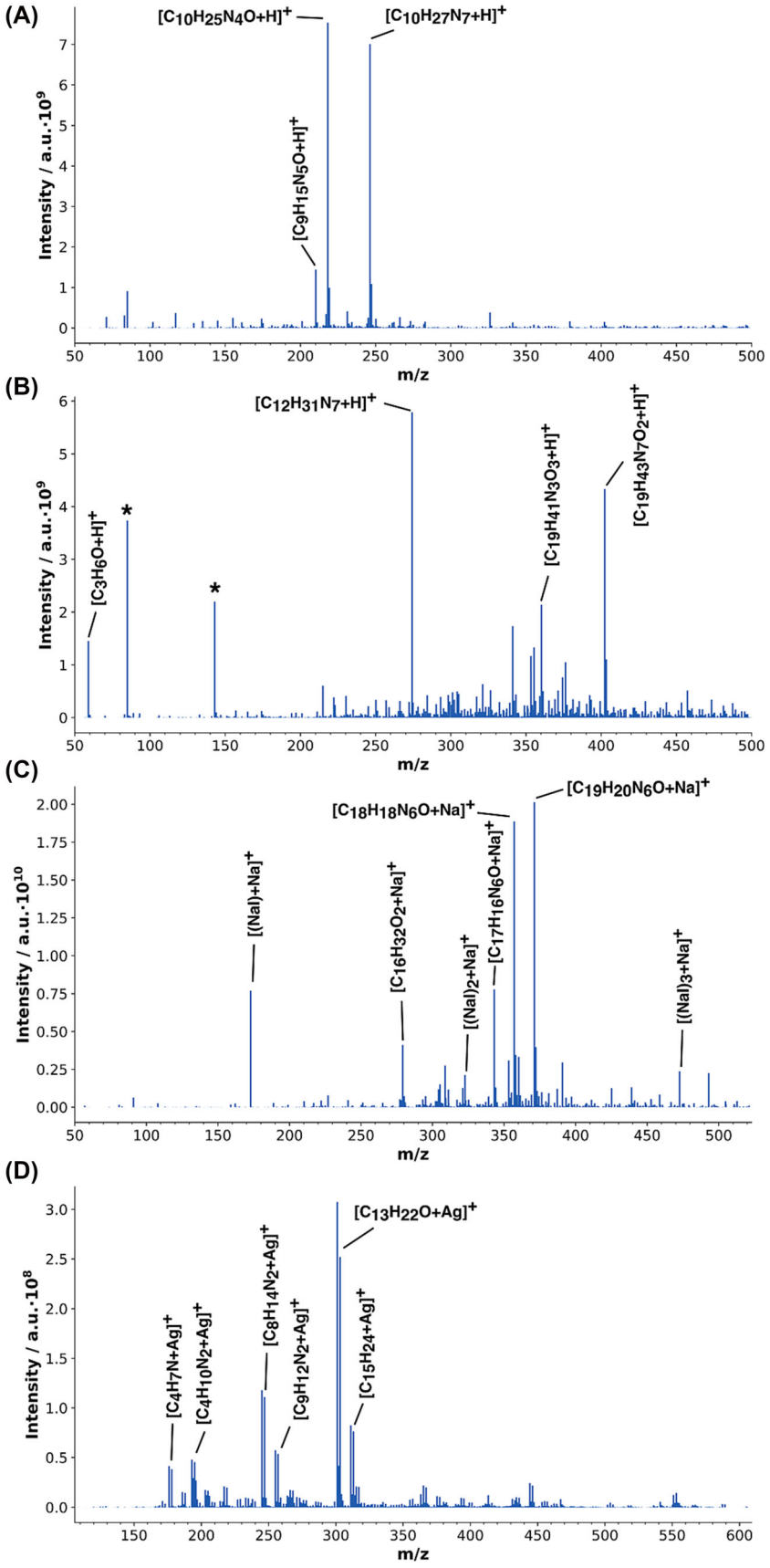

FIGURE 2 Average mass spectra over all three replicates, each consisting of six exhalations. For all electrolyte mixtures, a water–MeOH (50:50) mixture was the solvent of choice. (A) Solvent only, (B) FA, (C) NaI, and (D) $AgNO_3$. Selected peaks have been labeled with their molecular formula. Asterisk (*) indicates peaks that could not be assigned to a molecular formula. In contrast to the spectra shown in Figure 1, the most intense peaks were observed with the NaI-doped electrospray. For both FA and NaI, a shift in the more intense signals toward higher *m/z* ratios was observed compared to the spectra obtained using only water as solvent. [Color figure can be viewed at wileyonlinelibrary.com]

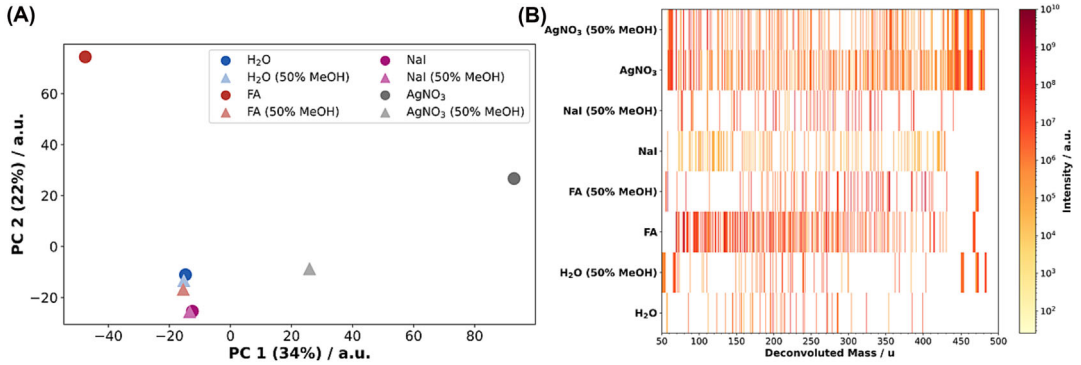

FIGURE 3 (A) First two principal components, along with their explained variance in all annotated molecular formulae and their corresponding intensity values. Data points marked by a circle indicate the data acquired with only water used as a solvent, whereas triangles denote data acquired with a water–MeOH (50:50) mixture. The first component differentiated the data obtained from the measurements with silver in the electrospray. (B) Distribution of the deconvoluted masses of the features found under the various electrospray conditions. FA in water and the silver-doped electrospray conditions both showed numerous intensive features. [Color figure can be viewed at wileyonlinelibrary.com]

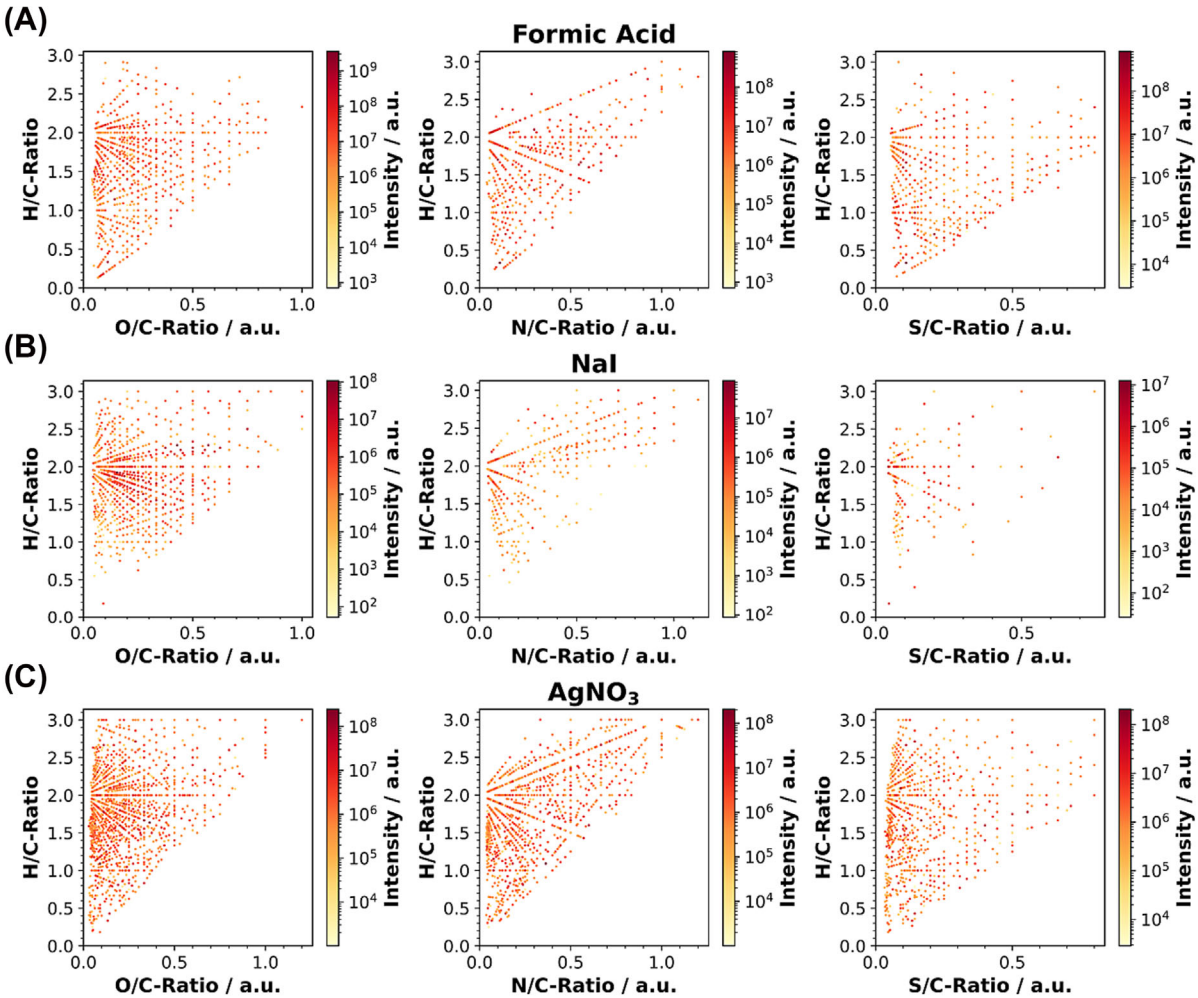

FIGURE 4 van Krewelen diagrams for (A) formic acid, (B) NaI, and (C) $AgNO_3$ electrospray data with water used as solvent. Compounds without the corresponding heteroatoms were not included. Although silver data generally showed a higher number of features, it also demonstrated clustering at low heteroatom ratios specifically around hydrogen–carbon ratios of 0.5 and 1.5. [Color figure can be viewed at wileyonlinelibrary.com]

conditions. The number of sulfur atoms within most compounds also seemed to be low. For all three doped electrosprays, the majority of features possessed an S–C ratio of less than 0.1, with only a few features annotated with molecular formulae with more than two sulfur atoms. This is congruent with the known classes of sulfur-containing compounds reported for exhaled breath.[37] Representing the data obtained with the MeOH-containing electrospray solutions similarly did not reveal significant differences (see van Krewelen diagram in Figure S2). Fewer features were detected when MeOH was incorporated within the electrospray.

Among the electrospray compositions tested, $AgNO_3$ appeared to provide the most comprehensive coverage of compounds present in exhaled breath.

3.3 | Gas standards

To further characterize the different electrolyte dopants, a series of chemicals were employed, including limonene (2.5 parts per billion [ppb]), eucalyptol (2.5 ppb), isopropanol (2.2 ppb), acetone (2.3 ppb), pentanoic acid (2.2 ppb), and pyridine (2.8 ppb). This selection covered a part of compound classes typically present in exhaled breath.[37] Initially, each compound was individually tested by increasing the compound's concentration linearly under both dry and humid conditions. Limonene was detected only with FA under dry conditions as the $[M + H]^+$ ion. No related signals were observed for the other dopants and conditions. Conversely, eucalyptol was detected with FA under both conditions and with silver in dry conditions. However, with silver dopant, the corresponding silver adduct for eucalyptol was not observed. Instead, the $[M + H]^+$ ion was obtained. Isopropanol produced a signal only with silver-doped electrospray and in dry conditions in the evaporation system, resulting in the $[M + Ag]^+$ ion. Acetone, on the contrary, was consistently detected under all conditions except for the silver-doped spray, with the acetone gas having been humidified. Regardless of the employed dopant, the $[M + H]^+$ ion was the major signal detected. Only with the sodium-doped spray and a humid dilution gas was a fraction observed as the $[M + Na]^+$ ion. Pentanoic acid yielded the $[M + H]^+$ ion with FA under dry and humid conditions. The NaI-doped spray was not capable of producing any observable signal. With $AgNO_3$, both the $[M + Ag]^+$ and $[M + H]^+$ ions were formed when the dilution gas was dry. These ions were not detected when the gas flow was humidified. Pyridine was the only compound for which, under all conditions, an ion was detected. Regardless of the electrospray dopant, the $[M + H]^+$ ion was formed. With silver, the adduct $[M + Ag]^+$ was also observed.

The measurements with the gas standards indicated that even with adduct-forming dopants, the compounds were detected in the form of $[M + H]^+$. Occasionally, adducts were an additional observed signal but were not the major species. Isopropanol was the only exception, which, when diluted with a dry gas flow, formed only the adduct with silver. No $[M + H]^+$ ions for isopropanol were observed under the tested conditions. This suggests that for the compounds tested and likely their broader classes, the protonated analyte is to be expected when employing adduct-forming dopants. This would explain why the breath measurements with an NaI-doped electrospray showed a less broad feature coverage. It is plausible that many of the signals detected with an NaI-doped spray corresponded to the protonated analyte. Because more breath features were detected as a silver adduct when using $AgNO_3$, different compound classes present in breath were likely ionized.

To further assess the sensitivities toward the tested gas standards, a mixture of all standards was analyzed, with a humid dilution flow (~95% relative humidity) mimicking exhaled breath conditions. The three different dopants tested in both aqueous and water–MeOH solutions, with the corresponding signal responses, are shown in Figure 5.

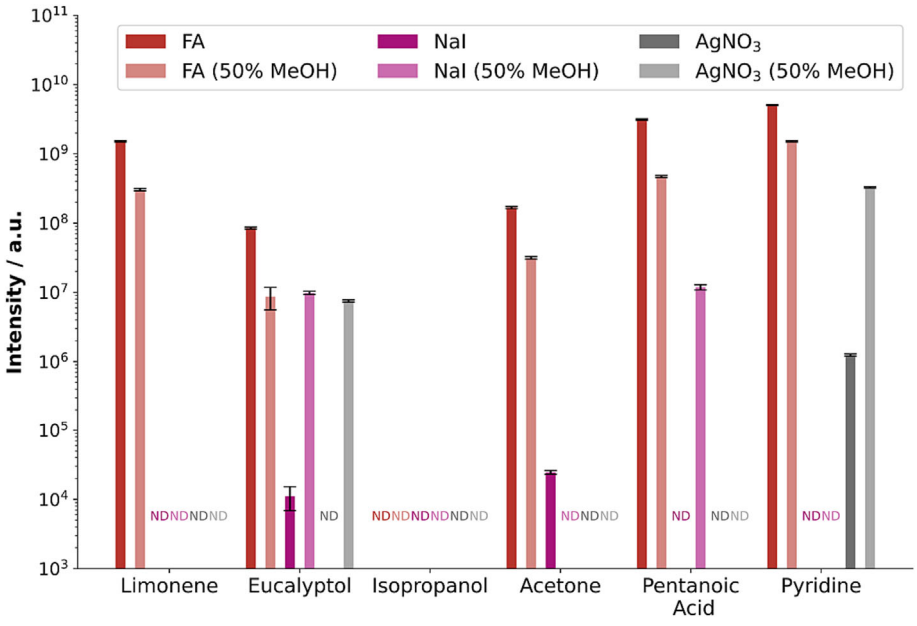

FIGURE 5 Intensities of the detected gas standard signals. For each electrospray condition, the signal of the expected adduct was taken. ND denotes conditions with no detected signal. For all tested compounds, the highest intensities were achieved with formic acid as an electrospray dopant. The responses of the tested dopants, NaI and $AgNO_3$, were lower and depended on whether the solution contained MeOH. [Color figure can be viewed at wileyonlinelibrary.com]

The signal responses in Figure 5 clearly show FA as the most effective dopant. Throughout the measurements, FA in water exhibited stronger responses compared to when it was dissolved in the water–MeOH mixture. The results for eucalyptol were surprising because compared to the results presented in Table S3, the adduct signals for NaI and for $AgNO_3$ in 50% MeOH were detected. It seems that for NaI in water, the concentration of the $[M + Na]^+$ ion surpassed the limit of detection, potentially due to spray variation. With MeOH added to the spray solution, for both sodium and silver, the corresponding adduct was more preferentially formed or even detected, respectively. In contrast, isopropanol did not elicit any signal response, even when tested with the water–MeOH mixture. Acetone exhibited a detectable response only with FA and NaI in water. In the case of pentanoic acid, it was almost the same, but instead of NaI in water, it was the MeOH mixture for which the adduct signal was observed. Finally, for pyridine, silver adducts could be observed with $AgNO_3$.

These results demonstrated strong sensitivity variances among the different spray dopants. Additionally, it was critical for NaI and $AgNO_3$ whether the spray solution consisted of pure water or a mixture of water–MeOH. The different responses of NaI and $AgNO_3$ to the measured compounds might have been influenced by the affinities of the cations Na^+ and Ag^+ toward water, MeOH, and the analyte molecules.[39] However, the obtained data do not allow for definite conclusions about the underlying mechanistic processes. It is, therefore, unclear whether the adduct-forming mechanism follows more an extractive process or gas-phase reactions.[15,40–42]

4 | CONCLUSIONS

To explore alternative electrolyte compositions for exhaled breath analysis using SESI-HRMS, breath measurements were conducted utilizing FA, NaI, and $AgNO_3$-doped electrospray solutions. An evaporation-based gas generation system was also used to measure the response of certain compounds to these electrospray compositions. When $AgNO_3$ was added to the electrospray, different metabolite classes were covered compared to the conventional FA dopant. With NaI, fewer features were detected, and compared to FA, the covered metabolite classes were not unique. Exploration of the annotated formulae of all features revealed the increased detection of features containing sulfur with silver. With a silver-doped electrospray, more features connected to unsaturated hydrocarbons and primary amines were detected as well. Using a mixture of water and MeOH for the electrospray solution did not improve feature detection, as more unique features were obtained with only water as the spray solvent.

The evaluation of compound sensitivities demonstrated that the strongest signal responses were obtained with FA-doped electrosprays. The efficacy of the other dopants was mixed, with some compounds not detected at all. For the tested compounds and their related compound classes, the widely used FA electrospray is still the optimal choice. NaI under the tested condition did not provide significant advantages and is, therefore, not an interesting alternative. On the contrary, $AgNO_3$ showed a different coverage of metabolites, and through the silver isotopic pattern, filtering of features is easily performed.

Water-based solvents are environmentally friendly and cost effective due to their abundance and nontoxicity. In contrast, MeOH is toxic and flammable, raising environmental and safety concerns. However, renewable MeOH can be greener. Regarding the costs of the individual solutions, water as a solvent is less expensive than MeOH, which would favor the water-only electrolyte solutions. Among dopants, $AgNO_3$ is the most expensive, followed by NaI. In terms of cost, the commonly employed FA-doped electrospray is the most economical. But the amount of dopant needed is minimal, and the used volume of the electrolyte solution is low. This minimizes the contribution toward operating costs and makes the cost a negligible factor.

Overall, $AgNO_3$ is an interesting dopant alternative or addition for exhaled breath analysis using SESI-HRMS. Although FA is effective, it is certainly worth conducting tests using $AgNO_3$ to discover additional biomarkers in exhaled breath.

AUTHOR CONTRIBUTIONS

Cedric Wüthrich and Stamatios Giannoukos designed the experiments. Cedric Wüthrich conducted the experiments and analyzed the data. Cedric Wüthrich, Stamatios Giannoukos, and Renato Zenobi interpreted the results. The manuscript was written with the contributions from all authors. All authors have approved the final version of the manuscript.

ACKNOWLEDGMENTS

This study has received funding from Agroscope (NutriExhalomics project, grant agreement no.: 15668) and the Ascher Trust. Open access funding provided by Eidgenossische Technische Hochschule Zurich.

CONFLICT OF INTEREST STATEMENT

The authors declare no conflicts of interest.

PEER REVIEW

The peer review history for this article is available at https://www.webofscience.com/api/gateway/wos/peer-review/10.1002/rcm.9714.

DATA AVAILABILITY STATEMENT

The original data used in this publication are made available in a curated data archive at ETH Zürich (https://www.research-collection.ethz.ch) under the DOI: 10.3929/ethz-b-000646253.

ORCID

Stamatios Giannoukos https://orcid.org/0000-0002-5066-533X

REFERENCES

1. Bruderer T, Gaisl T, Gaugg MT, et al. On-line analysis of exhaled breath. *Chem Rev*. 2019;119(19):10803-10828. doi:10.1021/acs.chemrev.9b00005
2. Schwarz EI, Sinues PML, Bregy L, et al. Effects of CPAP therapy withdrawal on exhaled breath pattern in obstructive sleep apnoea. *Thorax*. 2016;71(2):110-117. doi:10.1136/thoraxjnl-2015-207597
3. Streckenbach B, Osswald M, Malesevic S, Zenobi R, Kohler M. Validating discriminative signatures for obstructive sleep apnea in exhaled breath. *Cell*. 2022;11(19). doi:10.3390/cells11192982
4. Bregy L, Nussbaumer-Ochsner Y, Martinez-Lozano Sinues P, et al. Real-time mass spectrometric identification of metabolites characteristic of chronic obstructive pulmonary disease in exhaled breath. *Clin Mass Spectrom*. 2018;7:29-35. doi:10.1016/j.clinms.2018.02.003
5. Gaugg MT, Nussbaumer-Ochsner Y, Bregy L, et al. Real-time breath analysis reveals specific metabolic signatures of COPD exacerbations. *Chest*. 2019;156(2):269-276. doi:10.1016/j.chest.2018.12.023
6. Gaisl T, Bregy L, Stebler N, et al. Real-time exhaled breath analysis in patients with cystic fibrosis and controls. *J Breath Res*. 2018;12(3):036013. doi:10.1088/1752-7163/aab7fd
7. Weber R, Haas N, Baghdasaryan A, et al. Volatile organic compound breath signatures of children with cystic fibrosis by real-time SESI-HRMS. *ERJ Open Res*. 2020;6(1):00171-02019. doi:10.1183/23120541.00171-2019
8. Weber R, Streckenbach B, Welti L, et al. Online breath analysis with SESI/HRMS for metabolic signatures in children with allergic asthma. *Front Mol Biosci*. 2023;10:1154536. doi:10.3389/fmolb.2023.1154536
9. Tejero Rioseras A, Singh KD, Nowak N, et al. Real-time monitoring of tricarboxylic acid metabolites in exhaled breath. *Anal Chem*. 2018;90(11):6453-6460. doi:10.1021/acs.analchem.7b04600
10. Nowak N, Gaisl T, Miladinovic D, et al. Rapid and reversible control of human metabolism by individual sleep states. *Cell Rep*. 2021;37(4):109903. doi:10.1016/j.celrep.2021.109903
11. Wüthrich C, de Figueiredo M, Burton-Pimentel KJ, et al. Breath response following a nutritional challenge monitored by secondary electrospray ionization high-resolution mass spectrometry. *J Breath Res*. 2022;16(4):46007. doi:10.1088/1752-7163/ac894e
12. Lan J, Parte FB, Vidal-de-Miguel G, Zenobi R. Secondary electrospray ionization. In: *Breathborne Biomarkers and the Human Volatilome*. Elsevier; 2020:185-199. doi:10.1016/B978-0-12-819967-1.00012-8
13. Dryahina K, Polášek M, Smith D, Španěl P. Sensitivity of secondary electrospray ionization mass spectrometry to a range of volatile organic compounds: ligand switching ion chemistry and the influence of Zspray™ guiding electric fields. *Rapid Commun Mass Spectrom*. 2021;35(22):1-15. doi:10.1002/rcm.9187
14. Kaeslin J, Wüthrich C, Giannoukos S, Zenobi R. How soft is secondary electrospray ionization? *J am Soc Mass Spectrom*. 2022;33(10):1967-1974. doi:10.1021/jasms.2c00201
15. Meier L, Schmid S, Berchtold C, Zenobi R. Contribution of liquid-phase and gas-phase ionization in extractive electrospray ionization mass spectrometry of primary amines. *Eur J Mass Spectrom*. 2011;17(4):345-351. doi:10.1255/ejms.1146
16. Bruderer T, Gaugg MT, Cappellin L, et al. Detection of volatile organic compounds with secondary electrospray ionization and proton transfer reaction high-resolution mass spectrometry: a feature comparison. *J Am Soc Mass Spectrom*. 2020;31(8):1632-1640. doi:10.1021/jasms.0c00059
17. García-Gómez D, Gaisl T, Bregy L, et al. Real-time quantification of amino acids in the Exhalome by secondary electrospray ionization–mass spectrometry: a proof-of-principle study. *Clin Chem*. 2016;62(9):1230-1237. doi:10.1373/clinchem.2016.256909
18. Chen H, Venter A, Cooks RG. Extractive electrospray ionization for direct analysis of undiluted urine, milk and other complex mixtures without sample preparation. *Chem Commun*. 2006;19(19):2042-2044. doi:10.1039/b602614a
19. Koyanagi GK, Blagojevic V, Bohme DK. Applications of extractive electrospray ionization (EESI) in analytical chemistry. *Int J Mass Spectrom*. 2015;379:146-150. doi:10.1016/j.ijms.2015.01.011
20. Meier L, Berchtold C, Schmid S, Zenobi R. Extractive electrospray ionization mass spectrometry—enhanced sensitivity using an ion funnel. *Anal Chem*. 2012;84(4):2076-2080. doi:10.1021/ac203022x
21. Li M, Ding J, Gu H, et al. Facilitated diffusion of acetonitrile revealed by quantitative breath analysis using extractive electrospray ionization mass spectrometry. *Sci Rep*. 2013;3:1205. doi:10.1038/srep01205
22. Swanson KD, Spencer SE, Glish GL. Metal cationization extractive electrospray ionization mass spectrometry of compounds containing multiple oxygens. *J Am Soc Mass Spectrom*. 2017;28(6):1030-1035. doi:10.1007/s13361-016-1546-2
23. Lopez-Hilfiker FD, Pospisilova V, Huang W, et al. An extractive electrospray ionization time-of-flight mass spectrometer (EESI-TOF) for online measurement of atmospheric aerosol particles. *Atmos Meas Tech*. 2019;12(9):4867-4886. doi:10.5194/amt-12-4867-2019
24. Chen H, Wortmann A, Zhang W, Zenobi R. Rapid in vivo fingerprinting of nonvolatile compounds in breath by extractive electrospray ionization quadrupole time-of-flight mass spectrometry. *Angewandte Chemie*. 2007;119(4):586-589. doi:10.1002/ange.200602942
25. Brown WL, Day DA, Stark H, et al. Real-time organic aerosol chemical speciation in the indoor environment using extractive electrospray ionization mass spectrometry. *Indoor Air*. 2021;31(1):141-155. doi:10.1111/ina.12721
26. Pagonis D, Campuzano-Jost P, Guo H, et al. Airborne extractive electrospray mass spectrometry measurements of the chemical composition of organic aerosol. *Atmos Meas Tech*. 2021;14(2):1545-1559. doi:10.5194/amt-14-1545-2021
27. Lan J, Kaeslin J, Greter G, Zenobi R. Minimizing ion competition boosts volatile metabolome coverage by secondary electrospray ionization orbitrap mass spectrometry. *Anal Chim Acta*. 2021;1150:338209. doi:10.1016/j.aca.2021.338209
28. Wüthrich C, Fan Z, Vergères G, Wahl F, Zenobi R, Giannoukos S. Analysis of volatile short-chain fatty acids in the gas phase using secondary electrospray ionization coupled to mass spectrometry. *Anal Methods*. 2023;15(5):553-561. doi:10.1039/D2AY01778D
29. Martens L, Chambers M, Sturm M, et al. mzML—a community standard for mass spectrometry data. *Mol Cell Proteomics*. 2011;10(1):1-7. doi:10.1074/mcp.R110.000133
30. Chambers MC, MacLean B, Burke R, et al. A cross-platform toolkit for mass spectrometry and proteomics. *Nat Biotechnol*. 2012;30(10):918-920. doi:10.1038/nbt.2377
31. Sueur M, Maillard JF, Lacroix-Andrivet O, et al. PyC2MC: an open-source software solution for visualization and treatment of high-resolution mass spectrometry data. *J Am Soc Mass Spectrom*. 2023;34(4):617-626. doi:10.1021/jasms.2c00323
32. Kind T, Fiehn O. Seven Golden rules for heuristic filtering of molecular formulas obtained by accurate mass spectrometry. *BMC Bioinf*. 2007;8(1):105. doi:10.1186/1471-2105-8-105
33. Pedregosa F, Varoquaux G, Gramfort A, et al. Scikit-learn: machine learning in python. *J Mach Learn Res*. 2011;12(85):2825-2830.
34. Law WS, Wang R, Hu B, et al. On the mechanism of extractive electrospray ionization. *Anal Chem*. 2010;82(11):4494-4500. doi:10.1021/ac100390t
35. Roussis SG, Proulx R. Molecular weight distributions of heavy aromatic petroleum fractions by ag+ electrospray ionization mass spectrometry. *Anal Chem*. 2002;74(6):1408-1414. doi:10.1021/ac011002k
36. Jackson AU, Shum T, Sokol E, Dill A, Cooks RG. Enhanced detection of olefins using ambient ionization mass spectrometry: Ag+ adducts

of biologically relevant alkenes. *Anal Bioanal Chem*. 2011;399(1):367-376. doi:10.1007/s00216-010-4349-5

37. Drabińska N, Flynn C, Ratcliffe N, et al. A literature survey of all volatiles from healthy human breath and bodily fluids: the human volatilome. *J Breath Res*. 2021;15(3):034001. doi:10.1088/1752-7163/abf1d0
38. Laszakovits JR, MacKay AA. Data-based chemical class regions for Van Krevelen diagrams. *J Am Soc Mass Spectrom*. 2022;33(1):198-202. doi:10.1021/jasms.1c00230
39. Hoyau S, Norrman K, McMahon TB, Ohanessian G. A quantitative basis for a scale of Na+ affinities of organic and small biological molecules in the gas phase. *J Am Chem Soc*. 1999;121(38):8864-8875. doi:10.1021/ja9841198
40. Wang R, Gröhn AJ, Zhu L, et al. On the mechanism of extractive electrospray ionization (EESI) in the dual-spray configuration. *Anal Bioanal Chem*. 2012;402(8):2633-2643. doi:10.1007/s00216-011-5471-8
41. Rioseras AT, Gaugg MT, Martinez-Lozano Sinues P. Secondary electrospray ionization proceeds via gas-phase chemical ionization. *Anal Methods*. 2017;9(34):5052-5057. doi:10.1039/C7AY01121K
42. Dryahina K, Som S, Smith D, Španěl P. Reagent and analyte ion hydrates in secondary electrospray ionization mass spectrometry (SESI-MS), their equilibrium distributions and dehydration in an ion transfer capillary: modelling and experiments. *Rapid Commun Mass Spectrom*. 2021;35(7):1-10. doi:10.1002/rcm.9047

SUPPORTING INFORMATION

Additional supporting information can be found online in the Supporting Information section at the end of this article.

How to cite this article: Wüthrich C, Zenobi R, Giannoukos S. Alternative electrolyte solutions for untargeted breath metabolomics using secondary-electrospray ionization high-resolution mass spectrometry. *Rapid Commun Mass Spectrom*. 2024;38(8):e9714. doi:10.1002/rcm.9714